Examining the Influence of Linkers and Tertiary Structure in the Forced Unfolding of Multiple-Repeat Spectrin Molecules

Sterling Paramore and Gregory A. Voth
Center for Biophysical Modeling and Simulation, and Department of Chemistry, University of Utah, Salt Lake City, Utah 84112-0850

ABSTRACT The unfolding pathways of multiple-repeat spectrin molecules were examined using steered molecular dynamics (SMD) simulations to forcibly unfold double- and triple-repeat spectrin molecules. Although SMD has previously been used to study other repeating-domain proteins, spectrin offers a unique challenge in that the linker connecting repeat units has a definite secondary structure, that of an α-helix. Therefore, the boundary conditions imposed on a double- or triple-repeat spectrin must be carefully considered if any relationship to the real system is to be deduced. This was accomplished by imposing additional forces on the system which ensure that the terminal α-helices behave as if there were no free noncontiguous helical ends. The results of the SMD simulations highlight the importance of the rupture of the α-helical linker on the subsequent unfolding events. Rupture of the linker propagates unfolding in the adjacent repeat units by destabilizing the tertiary structure, ultimately resulting in complete unfolding of the affected repeat unit. Two dominant classes of unfolding pathways are observed after the initial rupture of a linker which involve either rupture of another linker (possibly adjacent) or rupture of the basic tertiary structure of a repeat unit. The relationship between the force response observed on simulation timescales and those of experiment or physiological conditions is also discussed.

INTRODUCTION

Spectrin is a ~200-nm-long tetrameric protein filament which is a primary component of the erythrocyte cytoskeleton and is responsible for the cell's elasticity (1). The individual monomers of spectrin are composed of 17–20 repeating domains, called spectrin repeat units. Many simulation (2–6) and experimental studies, including x-ray crystallography (7–9), temperature- and urea-induced unfolding (10,11), and atomic force microscopy (AFM) (2,12–16), have been performed to examine how the structure of the spectrin filaments (and specifically that of the repeat units) contributes to the elasticity of the cell. The AFM experiments have been of particular interest since they are capable of providing information about the force response of single spectrin molecules. The force-extension curve obtained from these AFM experiments shows a characteristic sawtooth pattern, where the peaks have been attributed to the force needed to rupture individual spectrin repeat units. Our previous simulation work (5,6) on single spectrin repeat units highlighted the importance of the contiguous α-helical ''linker'', which connects the repeat units. It was shown that changes in the structure of the linker were responsible for the initial features of the force response and that rupture of the linker resulted in a drastic change in the material properties of spectrin. This article presents steered molecular dynamics (SMD) (17,18) simulations of double- and triple-repeat spectrin molecules which confirm some of the conclusions of the previous work and demonstrate how linker rupture propagates unfolding in the adjacent repeat units.

Each repeat unit of spectrin consists of ~106 amino acids (19,20), which fold into a coiled-coil of three antiparallel α-helices (7–9,21,22). The helices are labeled (from the N- to C-terminal ends) A, B, and C, where helix B is aligned antiparallel to helices A and C (see Fig. 1). The helices exhibit a repeating pattern of specifically placed hydrophobic and hydrophilic residues, known as the heptad repeat pattern (8,23), which stabilizes the tertiary structure of the repeat units. The heptad repeat pattern is of the form $(a\text{-}b\text{-}c\text{-}d\text{-}e\text{-}f\text{-}g)_n$, where the a and d sites are typically occupied by hydrophobic residues and the e and g sites are typically occupied by ionic or hydrophilic residues. The helices are aligned such that the hydrophobic heptad sites of one helix are in close proximity to the complementary hydrophobic heptad sites of the other helices. Recent x-ray crystallography studies (7–9) have revealed that the repeat units are connected by a contiguous α-helical linker such that helix C of one repeat unit is contiguous with helix A of the adjacent repeat unit. This makes a multiple-repeat spectrin molecule topologically distinct from other repeating-domain proteins studied with AFM and simulation, such as the immunoglobulin and fibronectin type III domains of titin (24–31). The linker which connects the repeating domains of titin is a random coil, and thus extension will only straighten the random coil and the domains would be expected to unfold independently. However, in the case of spectrin, the linker has a definite secondary structure which is contiguous with the repeat units, making any distinction between the linker and the adjacent repeat units ambiguous (6). Therefore, unfolding of the linker would be expected to affect unfolding of the repeat unit and vice versa.

Submitted June 11, 2006, and accepted for publication July 25, 2006.

Address reprint requests to Gregory A. Voth, Center for Biophysical Modeling and Simulation, and Dept. of Chemistry, University of Utah, 315 S. 1400 E. Rm 2020, Salt Lake City, UT 84112-0850. E-mail: voth@chem.utah.edu.

0006-3495/06/11/3436/10 $2.00

doi: 10.1529/biophysj.106.091108

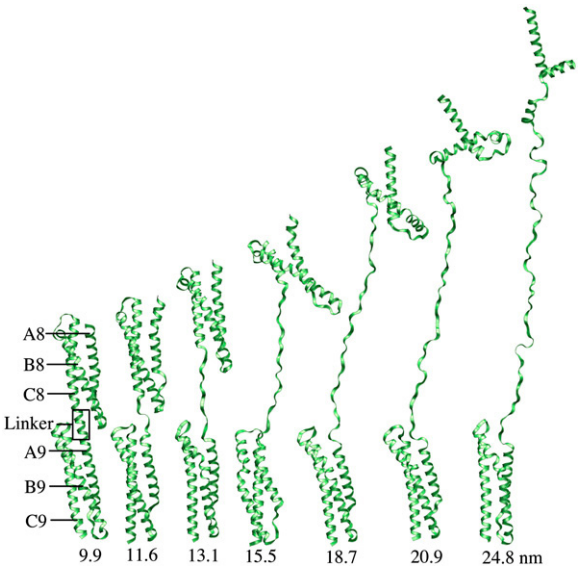

FIGURE 1 Sequence of structures for one of the SMD trajectories (the force-extension curve for this trajectory is shown in Figs. 2 *b* and 3 *b*).

The topology of multiple-repeat spectrins thus presents an interesting challenge for forced unfolding simulations (and experiment). To relate the behavior of just a few repeat units to the behavior of a full spectrin molecule, the boundary conditions imposed on the system must be carefully considered. Our previous work (5,6) utilized periodic boundary conditions to covalently attach a single spectrin repeat unit to its periodic image via a contiguous α-helical linker. The periodically replicated system corresponds to a long and perfectly straight chain of attached spectrin repeat units. Upon extension, a force peak was observed which was found to correspond to rupture of the hydrogen bonds maintaining the secondary structure of the α-helical linker. Although these boundary conditions were quite useful for probing the initial stages of rupture, they cannot be used to examine the subsequent unfolding behavior. This is because after the initial rupture event, the periodically replicated system corresponds to a long chain of spectrin repeat units where each repeat unit is surrounded by ruptured linkers, a situation not likely representative of either experimental or physiological conditions.

To examine how rupture of the linker connecting repeat units propagates unfolding in the adjacent repeat units, SMD simulations of both double- and triple-repeat spectrin molecules were performed. Of course, in a spectrin molecule composed of only a few repeat units (as is often studied in simulation and experiment) the terminal helices cannot form contiguous α-helical linkers, and thus would not be representative of the interior repeat units of a real 17–20 repeat spectrin monomer. Many of the effects of not having terminal α-helical linkers can be reincorporated by introducing artificial ''capping'' bonds on the terminal helices. As discussed in this article, this approach verifies that rupture of the linker plays a prominent role in the mechanism of spectrin unfolding under an applied force, at least on the timescales examined in this work. The effect that linker rupture has on the tertiary structure of the adjacent repeat units and the subsequent force response is also examined.

METHODS

All molecular dynamics simulations were performed with the NAMD simulation package (32) version 2.6b1 using the CHARMM22 (33) force field. Electrostatic interactions were treated with the particle mesh Ewald method using a tolerance of 1.0×10^{-6}. The nonbonded and real space parts of the electrostatic interactions were cut off at 12.0 Å. The SHAKE algorithm with a tolerance of 1.0×10^{-8} was used to constrain all bonds with hydrogen atoms and allowed for the use of a 2.0-fs time step. A Langevin piston with a period of 2 ps and a decay time of 1 ps was used to maintain system pressure at 1 atm. All atoms were subject to Langevin dynamics with a decay coefficient of 0.5 ps^{-1} and a temperature of 310 K. The CHARMM program (33) was used to construct and solvate the initial systems. Systems were solvated with an isotonic solution (0.155 M) of water, K^+, and Cl^- ions and subject to periodic boundary conditions. The SMD (17,18) technique, with a spring constant of 69.479 pN/Å, was used to extend the spectrin molecules.

Initial configurations for the double-repeat spectrin were based on a crystal structure of repeat units 8 and 9 of human erythroid β-spectrin (Protein Data Bank ID 1S35) (8). In the following discussion, the helices will be referred to as helix A8 for the A helix of repeat unit 8, helix B8 for the B helix of repeat unit 8, and helix C8A9 for the helix contiguous with repeat units 8 and 9 (likewise for repeat unit 9 and the triple-repeat structure). The system was solvated and equilibrated for 50 ns, as described in D. T. Mirijanian, J.-W. Chu, G. S. Ayton, and G. A. Voth (unpublished). When the system is subject to SMD, it is not allowed to rotate freely, and thus a large portion of the solvent needed for equilibration is not needed in the SMD simulations. Initial configurations for the SMD simulations were obtained by taking 10 configuration snapshots from the equilibrium simulation (spaced 1 ns apart), aligning spectrin along the z axis, and discarding solvent which did not fit into a simulation cell with dimensions of 53 Å in the x and y directions and 310 Å in the z direction. The final system sizes for the double-repeat SMD simulations were ~83,000 atoms.

In a real spectrin monomer, the native structure is composed of a sequence of 17–20 spectrin repeat units, thought to be attached to each other through contiguous α-helices (7–9,22,35,36). The simulations in this work examine spectrins consisting of only two or three of these repeat units. Of course, the terminal α-helices cannot be contiguous. Our earlier work (6) has suggested that rupture of the contiguous α-helical linker connecting repeat units is the initial, or nucleating, unfolding event and thus a careful examination of the appropriate boundary conditions is required. Other authors report simulations of single- and double-repeat spectrins which were extended by imposing forces on the terminal α-helices (2–4). But since the terminal α-helices were not contiguous, the systems examined were effectively adjacent to already ruptured linkers, making the interpretation of the subsequent unfolding dynamics somewhat ambiguous. However, some of the effects of having an adjacent repeat unit connected with a contiguous α-helical linker can be introduced by ''capping'' the terminal helices. Capping involves artificially changing the four α-helical hydrogen bonds nearest the terminal ends into purely harmonic interactions which cannot break. In this way, the terminal turns of the α-helices are always α-helical and the rest of the α-helix behaves as if it was part of a contiguous α-helix. In other words, for the helix to rupture, ~4 hydrogen bonds would need to rupture almost simultaneously; in contrast, a helix with free ends can unfold via sequential rupture of one hydrogen bond at a time starting from the free end. For this purpose, bonds with a spring constant of 650 kcal/mol/$Å^2$ and an equilibrium distance of 3.0 Å were added between the backbone O and N atoms of the four α-helix hydrogen

bond pairs nearest the terminal ends. All of the double-repeat simulations used capped terminal helices.

After solvation in the new simulation cell and addition of the artificial capping bonds, the system was equilibrated for 200 ps and then used in SMD simulations. SMD was applied by fixing the position of the N-terminal α-carbon atom and imposing the artificial harmonic SMD force to the C-terminal α-carbon.

Initial configurations for the triple-repeat simulations were obtained from a crystal structure of repeat units 15, 16, and 17 of chicken brain α-spectrin (Protein Data Bank ID 1U4Q) (9). Although this structure crystallized as a dimer, only the A segment and the surrounding waters were used for simulation. The triple-repeat spectrin was solvated with an isotonic solution in a truncated octahedron simulation cell with a principal axis width of 180 Å, giving a total system size of 463,995 atoms. The system was equilibrated in the constant NPT ensemble for 20 ns (using the Langevin dynamics described above), and the initial configurations for the SMD simulations were sampled from this equilibrium trajectory. Again, the SMD systems cannot freely rotate, and so all solvent molecules were discarded which did not fit into a simulation cell with dimensions of 62 Å in the x and y directions and 466 Å in the z direction (giving system sizes of ~172,000 atoms).

It was observed in the double-repeat simulations that the capped terminal helices did sometimes rupture (although not, of course, in the terminal turn). To avoid this situation in the triple-repeat simulations, no terminal helix capping was performed. Instead, the SMD forces were applied to the loops connecting helices A and B of the N-terminal repeat unit and helices B and C of the C-terminal repeat unit. In this case, force is not applied to the end linkers and thus it is not necessary that the end linkers form contiguous α-helices. It would not have been appropriate to impose the SMD forces in this manner on the double-repeat spectrin, because it restricts the number of possible unfolding pathways in the terminal repeat units, and in the double-repeat structure, both repeat units are terminal. However, in the triple-repeat structure, the central repeat unit is adjacent to two natural contiguous α-helical linkers. Imposing the SMD forces in this manner allowed for examination of how rupture of one linker affected the properties of a repeat unit which is adjacent to another natural contiguous α-helical linker.

The raw force data obtained from the SMD simulations is given as a function of time. Force-extension curves were obtained by binning the force data as a function of length. The error bars shown in some of the force-extension figures represent the standard deviation of the forces in a particular bin. This procedure can lead to artifacts due to poor sampling at the very beginning and end of the force-extension curves. Since the atom which is subject to the SMD steering potential vibrates in the potential, the force-extension curves are frequently artificially high at the beginning and artificially low at the end. Furthermore, although a plot of the force versus time does show that the system started at zero force (as would be expected, since the configurations were sampled from an equilibrium distribution), few of the force-extension curves show an initial force of zero. When the SMD potential starts to move, the force rises; but there can be some delay between this rise in force and a change in the length of the molecule. Therefore at short extensions, the average of the force response at a given length can be nonzero.

Most of the analysis of the resulting SMD trajectories was performed using the Tcl scripting capabilities of VMD (37). Disruption of the secondary structure of spectrin was measured by monitoring the maximum number of sequentially nonhelical residues (MNSNR) in a given region which forms an α-helix in the native structure. A residue was counted as being in an α-helical conformation if its backbone ϕ,ψ angles were $-105° \leq \phi \leq -25°$ and $-72° \leq \psi \leq -2°$. Hydrophobic surface area exposure was measured using the program MSMS (38).

Disruption of the tertiary structure of spectrin was analyzed by measuring the distance between complementary hydrophobic heptad sites. The proper hydrophobic heptad interactions are those between the d sites of helix A and the d sites of helix B, the a sites of helix A and the d sites of helix C, and the a sites of helix B and the a sites of helix C (8,23). For each SMD simulation, the initial configuration was taken as a reference; if the distance between complementary heptad sites of this reference structure was <12.0 Å, then the distance between those sites was monitored throughout the simulation. This information was plotted versus the total length of spectrin and the z position of the centroid of the heptad interaction in the reference structure. By plotting the interaction distances with reference to their initial position, disruption of the tertiary structure relative to the native structure can more easily be inferred.

It was also informative to measure bending undulations in the triple-repeat simulations. The angle between repeat units was defined through the use of a rotation matrix which minimized the root mean-squared distances between the α-carbons of two repeat units. The rotation matrix can be found using standard Tcl scripts in VMD (39). Once the matrix is found, a vector is defined which originates in the geometrical center of one repeat unit and terminates in the center of the other repeat unit. The vector is then rotated by the best-fit rotation matrix found above, and the angle between the repeat units is defined through the dot product of the original and rotated vectors.

RESULTS

The relationship between the structure of spectrin and the force-extension behavior was examined by measuring the contiguous nonhelicity (i.e., MNSNR) of the individual α-helices of spectrin, the distance between heptad interactions, and the hydrophobic surface area exposure. As will be shown in this section, nearly all of the major features of the force-extension curves are directly correlated with either sharp changes in the helicity or tertiary structure. Most of the following discussion will be concerned with the double-repeat simulations, as more data was collected and a more thorough statistical analysis could be performed. A sequence of configurations is shown for one of the double-repeat SMD simulations in Fig. 1.

Basic features of the force response

A total of 25 SMD trajectories of the double-repeat spectrin were obtained. Ten of the trajectories were propagated using pulling speeds of 2.0 nm/ns, 10 at 0.5 nm/ns, and 5 at 0.2 nm/ns. In all of the trajectories, the force quickly rises and peaks when it is extended by 0.5–1.0 nm (similar to the previous work (6), where a single spectrin repeat unit was subject to periodic boundary conditions). Beyond this initial feature, the force-extension curves show a number of different force peaks and sharp force drops, where the location of these features varies wildly between trajectories and appears to be placed at random. Given this wide range of force responses, it is not useful to examine averaged force-extension curves, as done previously (5,6). Instead, each force-extension curve must be considered independently. The collection of the individual responses can then be used to identify any general trends in the relationship between the structure of spectrin and its force response. Of the 25 force-extension curves examined, only 4 will be presented in this article (2 at 0.5 nm/ns and 2 at 0.2 nm/ns, see Fig. 2) but many others can be found in the Supplementary Material.

At the fastest pulling speeds examined, 2 nm/ns, the initial rise in the force-extension curve peaks at 510 ± 35 pN (average of all initial peaks at 2 nm/ns; unless otherwise

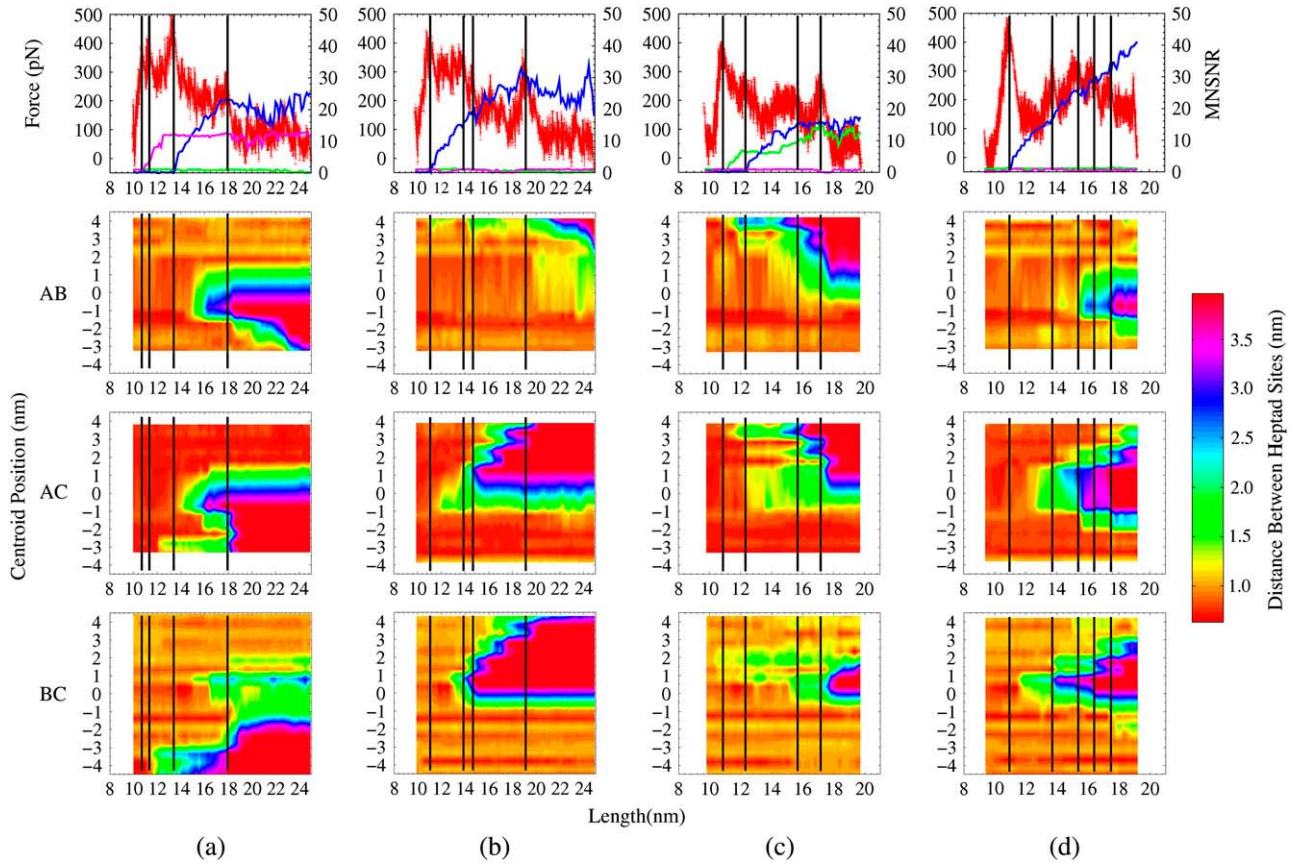

FIGURE 2 Correlation between the force-extension curve, the secondary structure, and the tertiary structure. The top row shows the force-extension curve (*left axis*, where the error bars are the standard deviation of the forces measured at a particular length) and the MNSNR (*right axis*, *green line* is helix A8, *blue* is helix C8A9, and *purple* is helix C9). The other figures are contour plots showing the distance between complementary heptad sites on the helices indicated on the left. Lines have been drawn to highlight the correlation between the force peaks and the tertiary structure. *a* and *b* were subject to a pulling speed of 0.5 nm/ns, and *c* and *d* were subject to a pulling speed of 0.2 nm/ns.

indicated, all error bars in this article are reported at the 95% confidence interval). At these speeds, the subsequent drop in the force response is fairly minimal and in many cases resembles a plateau more than a peak. The forces are only slightly less than that of the initial force peak until essentially complete rupture of a repeat unit occurs. These large forces are likely due to a strong viscous effect after rupture, as was observed at these pulling speeds in the previous work (6).

At the slower pulling speeds of 0.5 nm/ns, the initial force peak (370 $\pm$ 40 pN) is significantly smaller and the subsequent force drop is more pronounced. This indicates that the viscous forces which follow the initial rupture event have decreased with changes in pulling speed more than the rupture force. Over the next 4–10 nm of extension, a plateau region is usually observed and can consist of many smaller peaks.

When the pulling speed is further decreased to 0.2 nm/ns, the qualitative features of the force-extension curve are similar to the trajectories propagated at a pulling speed of 0.5 nm/ns. The initial force peak of 330 $\pm$ 80 pN is slightly less than the force peak at 0.5 nm/ns, although with only five trajectories, the difference is not statistically significant. There is also a small decrease in all subsequent forces.

Rupture of the secondary structure

In every trajectory examined, the initial force peak can be attributed to rupture of the secondary structure of either the central α-helical linker or the terminal helices. Fig. 2 shows the relationship between the force-extension curves and the MNSNR in the A8, C8A9, and C9 helices. It is observed that the first peak in the force-extension curves is always accompanied by a sharp increase in the MNSNR of one of these helices.

Although the terminal α-helices are not actual linkers, the capping bonds force the terminal turn of the α-helix to always stay in an α-helical conformation and thus mimic some of the effects of having a contiguous α-helical linker. For this reason, the terminal α-helices may also be referred to here as terminal linkers, although they are not strictly linkers. The only place the terminal linkers can rupture is a bit closer to the core of the repeat unit than an actual linker. The helices

are more stabilized in this region due to the presence of the heptad repeat pattern and would be expected to rupture less frequently than the central linker. This trend was observed; of the 15 SMD trajectories at pulling speeds of 0.5 and 0.2 nm/ns, only four involve rupture of the terminal linkers before rupture of the central linker. In all trajectories, the central linker did rupture at some point. Furthermore, in all instances where a linker ruptured, a force drop was also observed.

The force-extension curves also reveal that when only one linker has ruptured, the subsequent force peaks are larger than those where two linkers have ruptured. For example, in the 0.5 nm/ns-simulations, the first peak after rupture of a linker which cannot be attributed to rupture of another linker is 320 ± 40 pN (eight observations), whereas the first peak after rupture of a second linker is 240 ± 50 pN (four observations), a difference which is statistically significant. At 0.2 nm/ns, the force peaks are 240 ± 120 pN (two observations) and 190 ± 150 pN (three observations), respectively, which shows the same trend, although there were not enough observations for statistical significance. These results suggest that rupture of the linkers surrounding a repeat unit tend to destabilize it, making the repeat unit less able to resist external force and more likely to completely unfold.

Rupture of the tertiary structure

Nearly all of the peaks which cannot be attributed to rupture of a linker are highly correlated with changes in the tertiary structure. Tertiary structure changes were measured by monitoring the distance between complementary heptad sites, as discussed in the Methods section. The results can be seen in the contour plots of Fig. 2. In these contour plots, the color indicates the distance between hydrophobic heptad sites on the helices indicated, the x axis is the length of the spectrin molecule, and the y axis is the initial z position of the centroid of an interacting pair of heptad sites. Spectrin is aligned and extended along the z direction and is oriented so that the linker is at $z = 0$, repeat unit 8 is at $z > 0$, and repeat unit 9 is at $z < 0$. Lines have been drawn at distinct force peaks or sharp force drops. The figures show that a sharp drop in the force is almost always followed soon afterward by a sharp increase in the distance between some heptad sites. Although the converse is not true, sharp changes in the tertiary structure can occur even when no noticeable force peak is observed. This demonstrates that there is a strong correlation between the features of the force-extension curve and changes in the tertiary structure. These tertiary rupture peaks are smaller than the linker rupture force peaks as the average tertiary rupture peaks at 0.5 nm/ns are 286 ± 22 pN and at 0.2 nm/ns are 236 ± 33 pN (which are statistically different than each other and are also statistically different than the peaks assigned to linker rupture).

In some cases, a sharp drop in the force-extension curve is correlated with changes in the tertiary structure as well as a sharp increase in the exposed hydrophobic surface area, as seen in Fig. 3 *b*. However, not all peaks show this correlation, and in general the increase in the hydrophobic residue exposure is more gradual. This indicates that most of the tertiary force peaks cannot be solely attributed to disruption of hydrophobic interactions but instead suggests that a more complex combination of transient hydrophobic, steric, ionic, or hydrogen bonding interactions are responsible.

It can be tempting to assign some of these peaks to rupture of specific heptad interactions, as a peak is often correlated

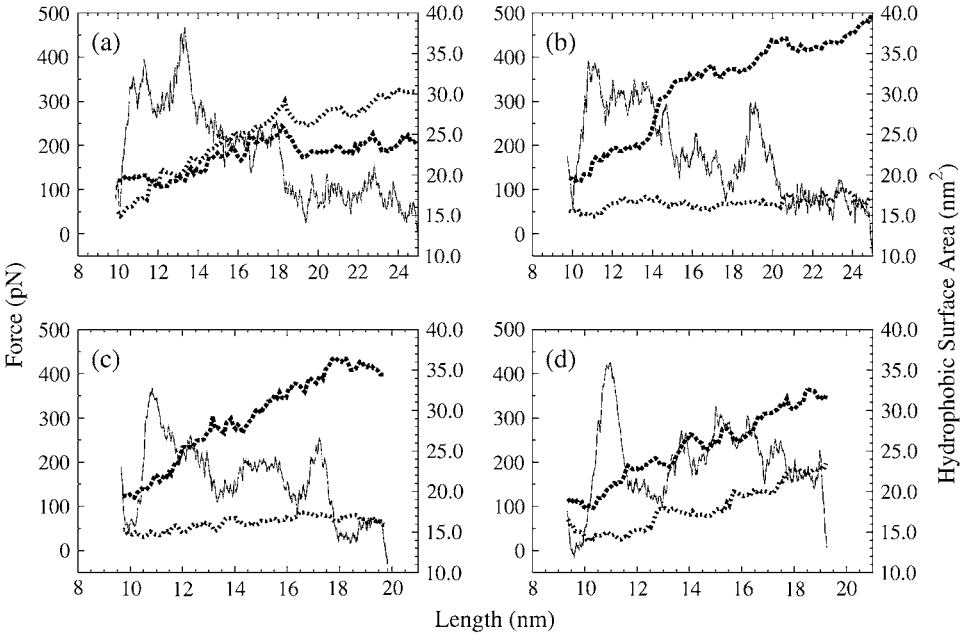

FIGURE 3 Correlation between the force-extension and the hydrophobic surface area exposure. The solid lines are the force-extension curves (*left axis*); the long and short dashed lines are the hydrophobic surface area exposure for repeat unit R8 and R9, respectively (*right axis*). *a* and *b* were subject to a pulling speed of 0.5 nm/ns, and *c* and *d* were subject to a pulling speed of 0.2 nm/ns. Error bars on the force-extension curve have been removed for clarity.

with a sharp change in the distance between two specific heptad sites. However, no specific localized tertiary rupture event was observed to consistently give rise to a force peak (at least, not as can be determined with the relatively small sample size available). With such a large variability in unfolding pathways, it is not possible to determine whether rupture of a localized heptad interaction is the source of the resistance to extension or if some other aspect of the structure changed under the stress and subsequently allowed rupture of the heptad interaction. Recall that the force measured using SMD decreases when the length of the spectrin molecule increases. Although an increase in length can sometimes be facilitated by a simple helix-coil transition, as discussed above, other times it requires more disperse conformational rearrangements. So although the peaks are correlated with localized changes in the distance between heptad sites, this change may sometimes only represent the last step in a series of more complex conformational adjustments.

Triple-repeat spectrin

Since there have been no reported simulations of a triple-repeat spectrin, a short description of the 20-ns equilibrium trajectory is in order. In the original crystal structure (9), the triple-repeat spectrin formed a dimer, but the simulations were performed on only one of the triple-repeat spectrins. In the first 8 ns of simulation, the molecule developed a significant bend, as can be seen in Fig. 4. The bend is easily observed when comparing the orientations of repeat units 15 and 17, but less so when comparing any two adjacent repeat units. Over the course of the trajectory, the bend appears to oscillate with a period of ~10 ns. To best analyze how a bend in spectrin contributes to the force response, the starting configurations for the SMD simulations were sampled from the more bent configurations between 6 and 10 ns of the equilibrium run.

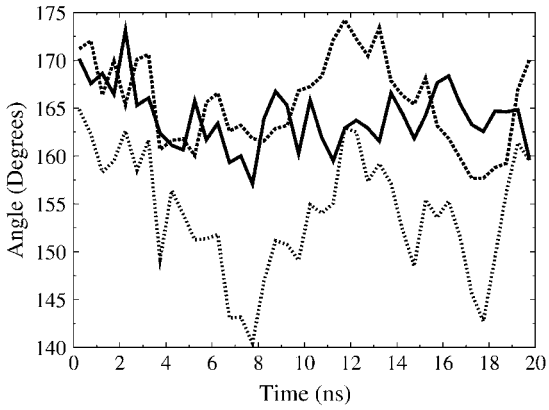

FIGURE 4 Angle between repeats 15 and 16 (*solid*), 16 and 17 (*long dash*), and 15 and 17 (*short dash*) of the triple-repeat chicken brain α-spectrin simulation.

Three SMD trajectories of the triple-repeat structure were obtained at a pulling speed of 0.5 nm/ns. The force response and unfolding behavior is very similar to that observed in the double-repeat simulations. In all three simulations, the force initially rises to 300–400 pN, at which point one of the linkers ruptures. Unfolding of this ruptured linker α-helix propagates into the adjacent repeat units until the other linker unfolds (see Fig. 5).

One important difference between these and the double-repeat simulations is the existence of a noticeable and significant bend. Fig. 6 shows the initial force-extension curve and angle between repeat units 15 and 17 for the three triple-repeat SMD simulations. At very short extensions, the angle between the terminal repeat units quickly increases, indicating that the structure is straightening out. The force-extension curve in the region where the largest changes in angle occur is essentially flat and constant at ~100 pN. The constant force is most likely due to a viscous effect, obscuring the conservative force response due to bending. This indicates that the force needed to straighten a multiple-repeat

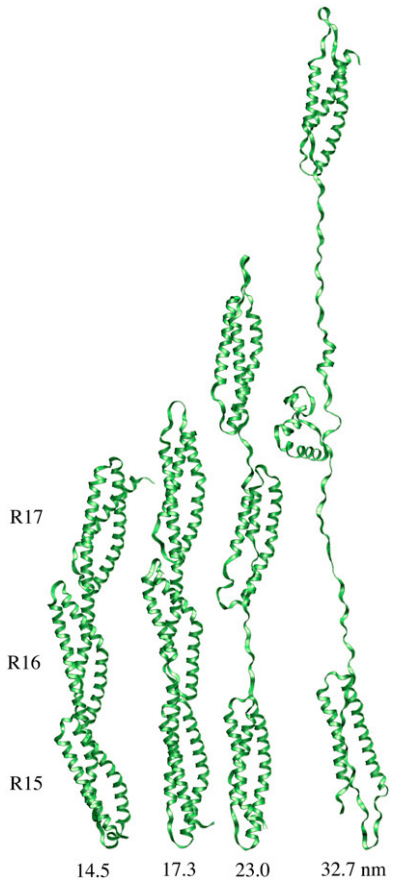

FIGURE 5 Sequence of structures for one of the triple-repeat SMD trajectories. The C15A16 linker ruptured at a length of 16.7 nm, and the C16A17 linker ruptured at 21.1 nm. Some rupture of the helices near the terminal loops was observed, but this is not expected to significantly affect the unfolding behavior of the central repeat unit.

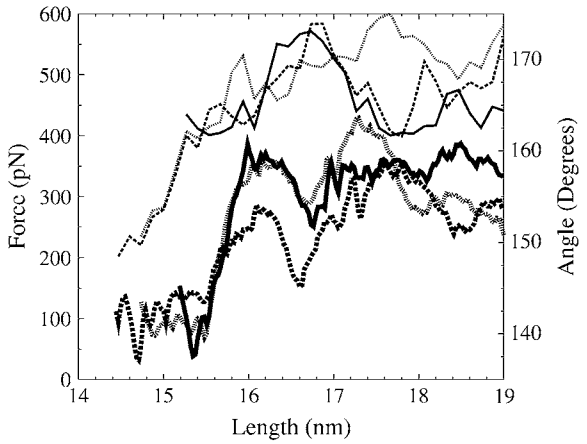

FIGURE 6 Initial force-extension curve (*thick lines*, *left axis*) and angle between repeat units 15 and 17 (*thin lines*, *right axis*) for three SMD simulations of the triple-repeat spectrin.

spectrin is essentially insignificant compared to the force needed to extend and rupture a repeat unit. This effect was also observed in some of the double-repeat simulations, although to a lesser extent (data not shown).

DISCUSSION

The simulations presented in this article confirm that linker rupture contributes to a substantial force peak (at least, on simulation timescales) and is not an artifact of the periodic boundary conditions or the method of linker construction used in the earlier work (6). As mentioned previously, the linker region is not stabilized by the tertiary heptad contacts and is thus the weakest point in the native structure; so it might be expected that rupture of the linker would be the initial unfolding event. When the system is extended beyond rupture of the linker, the helix-coil transitions propagate into the surrounding repeat units and disrupt the stabilizing heptad interactions in the hydrophobic core. In the double-repeat simulations, helix unfolding usually propagates more into repeat unit 8 than into repeat unit 9. In fact, complete repeat unit 9 unfolding was only observed when the C9 helix ruptured (i.e., only when both adjacent linkers unfold). This may indicate that, in general, helix C of a repeat unit is less stable and more prone to unfolding, or it could just be a subtle difference between repeat units 8 and 9 of human erythroid β-spectrin. Without being able to localize the critical tertiary rupture events, it is difficult to distinguish between the two possibilities and would require an analysis of unfolding of many different types of repeat units.

After the initial rupture of the linker and propagation of the helix-coil transitions into the adjacent repeat units, the precise rupture behavior varies dramatically between trajectories. This is a consequence of the fact that the entropy of an unfolded state is higher than that of the folded state. When spectrin unfolds, the structure is more disordered and has access to a large range of unfolding pathways. However, even though specific details of the unfolding pathways vary, it is still possible to identify two general classes of unfolding pathways which follow the initial unfolding event, as summarized in Fig. 7. 1), In some of the trajectories, the force rises to within ~100 pN of the initial linker rupture peak until an adjacent linker ruptures. After the second linker ruptures, the force is significantly smaller than the initial rupture event for the extensions examined. This is because after two linkers have ruptured, the repeat unit surrounded by those ruptured linkers is even more disordered, thereby giving it access to a wider range of unfolding pathways and is able to completely unfold at a lower force. 2), In other trajectories, the force will remain within ~100 pN of the initial linker rupture event until some tertiary interactions rupture. The force will then fall but in many cases can rise and fall again several times until essentially complete rupture of the tertiary structure has occurred.

In both cases, many of the trajectories finish with a force drop where the forces remain below 100 pN. These force drops are a consequence of rupture of some remaining tertiary interactions which result in essentially complete rupture of one of the repeat units. Rupture of tertiary interactions which result in a permanent force drop can occur over a wide range of extension, from lengths of 14 nm to >24 nm. Again, these rupture events cannot necessarily be localized to any specific residue-residue interactions, and many may be a result of more disperse conformational rearrangements. The

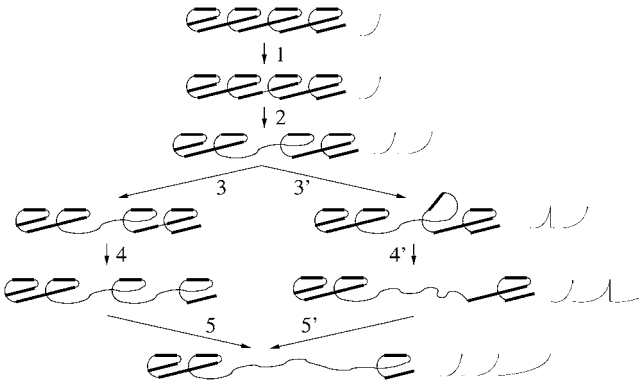

FIGURE 7 Schematic of the unfolding pathways of a quadruple-repeat spectrin, which are analogous to those actually observed in the simulations of double- and triple-repeat spectrins. Thick bars represent parts of the structure which are α-helical, and the thin bars represent sections which are random coils. To the right of each structure is a possible force-extension curve which might be observed over long timescales. The top structure shows the initial, fully folded spectrin molecule which has been extended to the point just before rupture. After rupture of the central α-helical linker (*1*), the force drops. As the system is extended (*2*), the force rises as unfolding of the linker propagates into the surrounding repeat units, disrupting the tertiary structure. When the force is large enough, either another linker can rupture (3), or the tertiary structure can completely unfold (*3′*). Either way, the repeat unit is highly destabilized and easily extensible (*4–5*, and *4′–5′*). Note that the trajectory shown in Fig. 1 follows the pathway on the right (*3′–5′*) and that shown in Fig. 5 follows the pathway on the left (*3–5*).

inability to localize many of these tertiary interactions is perhaps not surprising, given the low sequence homology of the repeat units (19) and complexity of the energy landscape (40–42). This suggests that the tertiary fold of spectrin is more of an influence on the force response than any specific residue-residue interactions.

Comparison with experiment

Due to the fact that the pulling speeds used in these simulations are up to six orders of magnitude faster than those used experimentally, a direct quantitative comparison of the forces and extensions is not appropriate. As discussed in the previous work (6), the unfolding pathways observed in the SMD simulations represent only the fastest unfolding pathways. There may also exist other, much slower unfolding pathways which cannot be observed on the timescale of the simulations but which may be significant on the timescales of experiment. Therefore, the results presented here are not intended to be quantitatively comparable to experiments. Instead, the following discussion is concerned with considering how the critical structural elements and fast pathways which were actually observed in the simulations might manifest on experimental timescales while acknowledging that alternative slower pathways could exist in conjunction with the fast ones.

Comparing these force-extension results with experiment is challenging not only due to the obvious differences between the simulation and experimental conditions, but also due to the fact that the few experiments which have been conducted are not in complete agreement. Some authors (12–14) report observing both single and tandem unfolding events. The forces needed for both of these events belong to the same force distribution of mean ~25 pN. Other authors (2,15) report observing short and long elongation events, where the short events are thought to be a consequence of a stable intermediate in the unfolding process. The force peaks of the short and long elongation events were found to belong to different distributions of mean ~60 pN and ~80 pN, respectively. The source of the discrepancies between these experiments is not entirely clear.

The force-extension curves derived from the SMD simulations discussed in this article show far more structure and much larger forces than any experimental results. This discrepancy is due, at least in part, to the much larger pulling speeds and shorter timescales used in the simulations. A key difference between the simulations and experiments concerns the nature of the thermal fluctuations encountered at the two timescales. Certain thermal fluctuations which are rare on simulation timescales can play a significant role on experimental timescales. Specifically, large force barriers observed in the SMD simulations can be dramatically reduced over longer timescales via those thermal fluctuations which act to extend the system in the same direction as the SMD biasing force (43). In this way, many of the force barriers observed in the SMD simulations would be expected to be smaller and could even be undetectable on experimental timescales.

The SMD simulations presented in this article show two classes of unfolding pathways which differ by the order in which tertiary and secondary structures rupture, as illustrated in Fig. 7. Both classes of unfolding pathways begin with rupture of a linker α-helix. Since the folded linker forms a contiguous structure with the adjacent repeat units, once it ruptures, the adjacent repeat units would be partially unfolded. An important question is whether these partially unfolded adjacent repeat units would be stable on submillisecond timescales before the structure is extended further. It has long been known that spectrin molecules consisting of only a few repeat units (i.e., those with noncontiguous linkers at the termini) fold into stable structures (9,11,20). Therefore, immediately after rupture of a single linker, the adjacent repeat units would be expected to maintain their basic tertiary structure on long timescales. However, it is not so clear what happens as the system is further extended. Fig. 3 implies that the hydrophobic forces which contribute to maintaining the folded structure only gradually change in response to continued extension. This suggests that the basic tertiary structure of a repeat unit may survive even after portions of the A or C helices have unfolded.

The SMD simulations have shown that the class of unfolding pathway that the system follows depends on a dynamic competition between rupture of critical secondary and tertiary structural elements. Given the above arguments concerning partially unfolded repeat units, some form of this competition is likely to exist even on experimental timescales, where thermal fluctuations could play a role in rupturing these structural elements. The simulations thus suggest that after rupture of a linker and further extension of the system, one of two things can happen (see Fig. 7). 1), Another linker, adjacent to the ruptured linker, could encounter a thermal fluctuation large enough to rupture it. As demonstrated with these simulations, once the surrounding linkers of a repeat unit have ruptured, exposure of the hydrophobic core is more easily facilitated and little additional force (compared to the force needed to rupture a linker) is needed to completely rupture the repeat unit. This conclusion is supported by the fact that temperature- and urea-induced unfolding experiments have shown that single repeat units are less stable than those with adjacent contiguously linked repeat units (9,11). 2), It is also possible that thermal fluctuations could rupture critical tertiary structure before rupture of another linker such that the repeat unit would be able to completely unfold. Complete unfolding of a repeat unit would necessarily rupture adjacent linkers which had not unfolded first, as the noncontiguous ends of the helices would no longer be stabilized by the fold of the spectrin repeat unit (the final configurations shown in Fig. 1 illustrate this effect). So the simulations suggest that the possible unfolding pathways after rupture of one linker involve either rupture of another linker which destabilizes the core of the repeat unit or rupture of the core of

the repeat unit which destabilizes the adjacent linkers. Both events would lead to the same peak-to-peak unfolding length and may not be differentiable in a traditional AFM experiment, as shown in Fig. 7.

Again, given the disparity between experimental and simulation timescales, it is not possible to determine which pathway might be dominant or even whether there might be alternative slower pathways which are more significant. However, this unfolding mechanism does have some interesting consequences. First of all, it would imply that the unfolding length between the first and second rupture events will be shorter than most of the other unfolding lengths. This is because in the initial structure, all linkers and repeat units are completely folded. The first rupture event would involve rupture of a linker which would propagate α-helix unfolding into the adjacent repeat units via helix-coil transitions. The next rupture event would involve this same gain in length but would in addition involve extension due to the completely ruptured repeat unit (that is, if the second rupture event involved rupture of a linker adjacent to the first ruptured linker). This effect is illustrated in Fig. 7. This mechanism is thus consistent with the fact that the short elongation events reported by Lenne et al. (15) were frequently (80% of the time) observed only early on in the unfolding process (where more of the linkers would be adjacent to two folded linkers).

The simulations do not suggest any physical mechanism by which a contiguous α-helical linker could couple two repeat units to simultaneously unfold, as suggested by other authors as an explanation for tandem events observed experimentally (3,12,14). However, consider the unfolding mechanism originally proposed by Rief et al. (16), where the unfolding events were thought to involve rupture of the hydrophobic core of the repeat unit before rupture of any secondary structure. This type of unfolding mechanism would require conformational transitions not likely to be observed on simulation timescales and would thus correspond to a slow unfolding pathway. As the simulations and Fig. 7 demonstrate, rupture of the core of the repeat unit necessarily disrupts the continuity and thus the stability of the adjacent linkers. Therefore, if a slow rupture event were to occur which involved this type of mechanism, it would necessarily rupture the two adjacent linkers and give rise to an unfolding length up to twice as long as any single linker rupture event would (see Fig. 8). For one of these slower rupture events to occur, the linkers would have to remain intact over a long period of time. At elevated temperatures, the α-helical linkers are less stable and more prone to rupture. Therefore, at high temperatures, these slow events would be less likely to occur before rupture of the linkers. This mechanism would be compatible with the observed temperature dependence of tandem unfolding (14), where fewer tandem events and less α-helicity are observed at higher temperatures. The higher temperatures destabilize the α-helical structure of the linkers, which would make the fast (and thus shorter) unfolding pathways more probable.

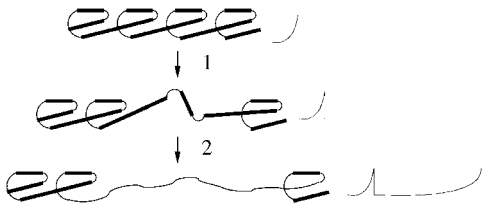

FIGURE 8 This figure shows a schematic for a possible unfolding mechanism which could account for the tandem unfolding events observed experimentally (12,14). Instead of helix rupture nucleating the unfolding, as shown in Fig. 7, a slow rupture pathway involving disruption of the coiled-coil fold might occur (*1*). This would result in destabilization of the two adjacent α-helical linkers and thus to an extra long unfolding event.

CONCLUSIONS

The goal of these simulations was to examine how multiple-repeat spectrin molecules unfold under an applied force. These simulations confirm our previous result, that linker unfolding can be the nucleating unfolding event and also provide some additional information. It was demonstrated that once a linker unfolds, helix-coil transitions propagate into the surrounding repeat units and destabilize the tertiary structure, thus opening up a wide range of unfolding pathways. As the system continues to be extended, there is dynamic competition between continued rupture of tertiary structure and rupture of another linker. Disruption of the tertiary structure may continue until the basic structure of the repeat unit is completely destroyed or until an adjacent linker ruptures. The unfolding pathways actually observed in the SMD simulations suggest an interesting unfolding mechanism which may occur on experimental timescales. This unfolding mechanism is consistent with both the simulation results presented as well as many features observed in AFM experiments.

SUPPLEMENTARY MATERIAL

An online supplement to this article can be found by visiting BJ Online at http://www.biophysj.org.

The authors would like to thank Dina T. Mirijanian for providing the equilibrium configurations of the double-repeat spectrin molecules.

This research was supported by a grant from the National Science Foundation Information Technology Research program (No. CHE-0218739). The computation resources for this work were partially supported by the National Science Foundation under grant No. MCA94P017N through TeraGrid resources provided by the National Center for Supercomputing Applications and the Pittsburgh Supercomputing Center.

REFERENCES

1. Elgsaeter, A., B. T. Stokke, A. Mikkelsen, and D. Branton. 1986. The molecular basis of erythrocyte shape. *Science*. 234:1217–1223.
2. Altmann, S. M., R. G. Grünberg, P.-F. Lenne, J. Ylänne, A. Raae, K. Herbert, M. Saraste, M. Nilges, and J. K. H. Hörber. 2002. Pathways

and intermediates in forced unfolding of spectrin repeats. *Structure*. 10:1085–1096.

3. Ortiz, V., S. O. Nielsen, M. L. Klein, and D. E. Discher. 2005. Unfolding a linker between helical repeats. *J. Mol. Biol.* 349:638–647.
4. Paci, E., and M. Karplus. 2000. Unfolding proteins by external forces and temperature: the importance of topology and energetics. *Proc. Natl. Acad. Sci. USA*. 97:6521–6526.
5. Paramore, S., G. S. Ayton, D. T. Mirijanian, and G. A. Voth. 2006. Extending a spectrin repeat unit. I: Linear force-extension response. *Biophys. J.* 90:92–100.
6. Paramore, S., G. S. Ayton, and G. A. Voth. 2006. Extending a spectrin repeat unit. II: Rupture behavior. *Biophys. J.* 90:101–111.
7. Grum, V. L., D. Li, R. I. MacDonald, and A. Mondragón. 1999. Structures of two repeats of spectrin suggest models of flexibility. *Cell.* 98: 523–535.
8. Kusunoki, H., R. I. MacDonald, and A. Mondragón. 2004. Structural insights into the stability and flexibility of unusual erythroid spectrin repeats. *Structure*. 12:645–656.
9. Kusunoki, H., G. Minasov, R. I. MacDonald, and A. Mondragón. 2004. Independent movement, dimerization and stability of tandem repeats of chicken brain α-spectrin. *J. Mol. Biol.* 344:495–511.
10. MacDonald, R. I., and J. A. Cummings. 2004. Stabilities of folding of clustered, two-repeat fragments of spectrin reveal a potential hinge in the human erythroid spectrin tetramer. *Proc. Natl. Acad. Sci. USA*. 101: 1502–1507.
11. MacDonald, R. I., and E. V. Pozharski. 2001. Free energies of urea and of thermal unfolding show that two tandem repeats of spectrin are thermodynamically more stable than a single repeat. *Biochemistry*. 40: 3974–3984.
12. Law, R., P. Carl, S. Harper, P. Dalhaimer, D. W. Speicher, and D. E. Discher. 2003. Cooperativity in forced unfolding of tandem spectrin repeats. *Biophys. J.* 84:533–544.
13. Law, R., S. Harper, D. W. Speicher, and D. E. Discher. 2004. Influence of lateral association on forced unfolding of antiparallel spectrin heterodimers. *J. Biol. Chem.* 279:16410–16416.
14. Law, R., G. Liao, S. Harper, G. Yang, D. W. Speicher, and D. E. Discher. 2003. Pathway shifts and thermal softening in temperature-coupled forced unfolding of spectrin domains. *Biophys. J.* 85:3286–3293.
15. Lenne, P.-F., A. J. Raae, S. M. Altmann, M. Saraste, and J. K. H. Hörber. 2000. States and transitions during forced unfolding of a single spectrin repeat. *FEBS Lett.* 476:124–128.
16. Rief, M., J. Pascual, M. Saraste, and H. E. Gaub. 1999. Single molecule force spectroscopy of spectrin repeats: low unfolding forces in helix bundles. *J. Mol. Biol.* 286:553–561.
17. Grubmüller, H., B. Heyman, and P. Tavan. 1996. Ligand binding: molecular mechanics calculation of the streptavidin-biotin rupture force. *Science*. 271:997–999.
18. Izrailev, S., S. Stepaniants, M. Balsera, Y. Oono, and K. Schulten. 1997. Molecular dynamics study of unbinding of the avidin-biotin complex. *Biophys. J.* 72:1568–1581.
19. Wasenius, V.-M., M. Saraste, P. Salvén, M. Erämaa, L. Holm, and V.-P. Lehto. 1989. Primary structure of the brain α-spectrin. *J. Cell Biol.* 108:79–93.
20. Winograd, E., D. Hume, and D. Branton. 1991. Phasing the conformational unit of spectrin. *Proc. Natl. Acad. Sci. USA*. 88:10788–10791.
21. Pascual, J., M. Pfuhl, D. Walther, M. Saraste, and M. Nilges. 1997. Solution structure of the spectrin repeat: a left-handed antiparallel triple-helical coiled-coil. *J. Mol. Biol.* 273:740–751.
22. Yan, Y., E. Winograd, A. Viel, T. Cronin, S. C. Harrison, and D. Branton. 1993. Crystal structure of the repetitive segments of spectrin. *Science.* 262:2027–2030.
23. Parry, D. A. D., T. W. Dixon, and C. Cohen. 1992. Analysis of the three-α-helix motif in the spectrin superfamily of proteins. *Biophys. J.* 61:858–867.
24. Krammer, A., H. Lu, B. Isralewitz, and V. Vogel. 1999. Forced unfolding of the fibronectin type III module reveals a tensile molecular recognition switch. *Proc. Natl. Acad. Sci. USA*. 96:1351–1356.
25. Lu, H., B. Isralewitz, A. Krammer, V. Vogel, and K. Schulten. 1998. Unfolding titin immunoglobulin domains by steered molecular dynamics simulation. *Biophys. J.* 75:662–671.
26. Lu, H., and K. Schulten. 1999. Steered molecular dynamics simulations of force-induced protein domain unfolding. *Proteins*. 35:453–463.
27. Lu, H., and K. Schulten. 2000. The key event in force-induced unfolding of titin's immunoglobulin domains. *Biophys. J.* 79:51–65.
28. Oberhauser, A. F., P. E. Marszalek, H. P. Erickson, and J. M. Fernandez. 1998. The molecular elasticity of the extracellular matrix protein tenascin. *Nature*. 393:181–185.
29. Paci, E., and M. Karplus. 1999. Forced unfolding of fibronectin type 3 modules: an analysis by biased molecular dynamics simulations. *J. Mol. Biol.* 288:441–459.
30. Rief, M., M. Gautel, F. Oesterhelt, J. M. Fernandez, and H. E. Gaub. 1997. Reversible unfolding of individual titin immunoglobulin domains by AFM. *Science*. 276:1109–1112.
31. Rief, M., M. Gautel, A. Schemmel, and H. E. Gaub. 1998. The mechanical stability of immunoglobulin and fibronectin III domains in the muscle protein titin measured by atomic force microscopy. *Biophys. J.* 75:3008–3014.
32. Kale, L., R. Skeel, M. Bhandarkar, R. Brunner, A. Gursoy, N. Krawetz, J. Phillips, A. Shinozaki, K. Varadarajan, and K. Schulten. 1999. NAMD2: greater scalability for parallel molecular dynamics. *J. Comput. Phys.* 151:283–312.
33. MacKerell, A. D. Jr., D. Bashford, M. Bellott, R. L. Dunbrack Jr., J. D. Evanseck, M. J. Field, S. Fischer, J. Gao, H. Guo, S. Ha, D. Joseph-McCarthy, L. Kuchnir, K. Kuczera, F. T. K. Lau, C. Mattos, S. Michnick, T. Ngo, D. T. Nguyen, B. Prodhom, W. E. Reiher 3rd, B. Roux, M. Schlenkrich, J. C. Smith, R. Stote, J. Straub, M. Watanabe, J. Wiorkiewicz-Kuczera, D. Yin, and M. Karplus. 1998. All-atom empirical potential for molecular modeling and dynamics studies of proteins. *J. Phys. Chem. B*. 102:3586–3616.
34. Reference deleted in proof.
35. Djinović-Carugo, K., P. Young, M. Gautel, and M. Saraste. 1999. Structure of the α-actinin rod: molecular basis for cross-linking of actin filaments. *Cell.* 98:537–546.
36. Ylänne, J., K. Scheffzek, P. Young, and M. Saraste. 2001. Crystal structure of the α-actinin rod reveals an extensive torsional twist. *Structure.* 9:597–604.
37. Humphrey, W., A. Dalke, and K. Schulten. 1996. VMD: visual molecular dynamics. *J. Mol. Graph.* 14:33–38.
38. Sanner, M. F., J.-C. Spehner, and A. J. Olson. 1996. Reduced surface: an efficient way to compute molecular surfaces. *Biopolymers*. 38: 305–320.
39. Kabsch, W. 1978. A discussion of the solution for the best rotation to relate two sets of vectors. *Acta Crystallogr.* A34:827–828.
40. Scott, K. A., S. Batey, K. A. Hooton, and J. Clarke. 2004. The folding of spectrin domains I: wild-type domains have the same stability but very different kinetic properties. *J. Mol. Biol.* 344:195–205.
41. Scott, K. A., and J. Clarke. 2005. Spectrin R16: broad energy barrier or sequential transition states? *Protein Sci.* 14:1617–1629.
42. Scott, K. A., L. G. Randles, and J. Clarke. 2004. The folding of spectrin domains II: phi-value analysis of R16. *J. Mol. Biol.* 344: 207–221.
43. Hummer, G., and A. Szabo. 2003. Kinetics from nonequilibrium single-molecule pulling experiments. *Biophys. J.* 85:5–15.